

Cross Section Analysis for Neutron and Proton Induced Reactions on ^{55}Mn Material

Mustafa Yiğit¹

Published online: 6 August 2015
© Springer Science+Business Media New York 2015

Abstract Nuclear data on structural materials are an important tool in the safe and efficient design of nuclear fusion reactors. Manganese is an important material because of low activation property for fusion reactors. Thus, the manganese metal is commonly used as a key component of many important alloys. And also, it is considered as the shielding materials for nuclear fusion reactor. In the present paper, the excitation functions of neutron and proton induced reactions on fusion structural material Manganese have been calculated by using Hybrid, Geometry Dependent Hybrid and Weisskopf Ewing models. In addition, the different nuclear level density models were tested such as Fermi Gas model with an energy independent level density parameter, and Fermi Gas model of Ignatyuk, Smirenkin, Tishin with an energy dependent level density parameter, and Superfluid nuclear model, and Kataria–Ramamurthy Fermi Gas model. The obtained theoretical cross section calculations in the framework of these nuclear models have been compared with the each other and, the experimental data and TENDL-2014 library. Finally, it seemed that the nuclear cross section calculations are quite sensitive to level densities for nucleon induced reactions.

Keywords Manganese · Weisskopf Ewing theory · Cross section · Kataria–Ramamurthy Fermi Gas model

Introduction

Nuclear fusion as an efficient source of energy offers the potential of numerous attractive features such as large-scale energy source, broadly available, including no emissions of greenhouse gases, no long-lived radioactive waste, and no risk of a severe accident [1]. The selection of appropriate structural materials for fusion reactors is one of the most important goals of nuclear technology. Manganese material is an important structural material for fusion reactors because of low activation property. It is used as a key component of many important alloys. Furthermore it is considered as the shielding materials for fusion devices [2, 3]. On the other hand, the nuclear data are an indispensable component of nuclear fusion devices, because they are an important tool in the safe and efficient design of nuclear fusion reactors. Particularly, the nuclear cross section data has a critical importance on the development of fusion reactor technology. If the experimental nuclear data are unavailable or unreliable, the modern theoretical theories are generally required for the estimation of the nuclear cross sections [4–7].

The nuclear reactions induced by nucleons are important for understanding the processes of the reaction mechanism and also to test the validity of nuclear models. The calculations via nuclear models require various physics inputs such as level densities, exciton numbers, nuclear masses, ground state deformations, particle optical potential models, discrete levels, γ -strength functions, fission barriers, and decay schemes. Especially, the nuclear level densities are required for a more detailed understanding of nuclear reaction processes and for the calculation of reaction cross sections. And also, the level densities are crucial parameters in various applications in nuclear science and technology such as fission and fusion reactors, astrophysics,

✉ Mustafa Yiğit
mustafayigit@aksaray.edu.tr

¹ Department of Physics, Faculty of Science and Arts, Aksaray University, Aksaray, Turkey

nuclear medicine and accelerator driven systems. Both theoretical and experimental investigations for improving the nuclear data have to be carried out. Nuclear level densities are required at excitation energy where discrete level information is not available or incomplete to get the theoretical analysis of nuclear reaction cross sections. Analytical level density formulas are still routinely used in nuclear reaction cross section calculations [7].

In the present paper, the cross sections of $^{55}\text{Mn}(n,4n)^{52}\text{Mn}$, $^{55}\text{Mn}(n,2p)^{54}\text{V}$, $^{55}\text{Mn}(n,^3\text{He})^{53}\text{V}$, $^{55}\text{Mn}(n,p\alpha)^{51}\text{Ti}$, $^{55}\text{Mn}(p,2n)^{54}\text{Fe}$, $^{55}\text{Mn}(p,3n)^{53}\text{Fe}$ and $^{55}\text{Mn}(p,4n)^{52}\text{Fe}$ nuclear reactions for the structural fusion material ^{55}Mn were calculated using four different level density models (Fermi Gas model with an energy independent level density parameter [8] and, Fermi Gas model of Ignatyuk, Smirenkin, Tishin with an energy dependent level density parameter [9] and, Superfluid nuclear model [10] and, Kataria–Ramamurthy Fermi Gas model [11]) by the code ALICE/ASH [8]. The calculated nuclear cross sections were compared with the each other and against the experimental data.

Cross Section Calculation Methods

The equilibrium and pre-equilibrium emissions of particles for a nuclear reaction can be calculated by the Weisskopf Ewing model [12] and, Geometry Dependent Hybrid [13] and Hybrid models [14, 15], respectively.

ALICE/ASH Code

The nuclear code ALICE/ASH was developed by Broeders et al. [8] as a modified version of the code ALICE-91 [16], which is useful for calculating of pre-equilibrium and equilibrium reaction processes. This nuclear reaction code includes the implementation of nuclear models describing the pre-equilibrium emission of composite particle, the fast γ -emission, and the model for the fission fragment yield calculation and different approaches for calculation of level densities. The ALICE/ASH as a nuclear reaction code is useful for calculation of the nuclear excitation functions, energies and angular distributions of secondary particles in reactions produced by nucleons and nuclei with the incident energy up to 300 MeV [8]. The GDH model is a version of the hybrid model, in which the nuclear geometry effects are taken into account. Also, it considers the shallow potential at the nuclear surface and hence also the reduced matter density [8]. The nuclear pre-compound process becomes increasingly important above 10–20 MeV and, the pre-compound effects play a dominant role at projectile energies above 50 MeV. Finally, at projectile energies above about 10–20 MeV the results of

calculations using the Geometry Dependent Hybrid model give a good agreement with experimental cross section data.

Fermi Gas Model Proposed by Ignatyuk, Smirenkin, Tishin with an Energy-Dependent Level Density Parameter

The level density is written by the expression

$$\rho(U) \propto a^{-1} A^4 (U - \delta)^{-5} e^{(2\sqrt{a(U-\delta)})} \tag{1}$$

The phenomenological expression for nuclear level density parameter usually referred to as the Ignatyuk formula is described as follows [9]

$$a(U) = \tilde{a} \left(1 + \frac{f(U)\delta W}{U} \right) \tag{2}$$

here the term δW is shell correction. The term \tilde{a} denotes the asymptotic value of the level density parameter and equal to $A(\alpha + \beta A)$.

$$f(U) = 1 - e^{(-\gamma U)}; \quad \beta = -6.3 \times 10^{-5}; \quad \alpha = 0.154; \\ \gamma = 0.054 \text{ MeV}^{-1}$$

The pairing correction δ is

$$\delta = 0 \quad \text{for odd-odd nuclei}$$

$$\delta = 12/A^{1/2} \quad \text{for nuclei with odd } A$$

$$\delta = 24/A^{1/2} \quad \text{for even-even nuclei}$$

At excitation energies < 2 MeV the level density is calculated using the constant temperature approach [8].

Superfluid Nuclear Model

The level density is written according to the generalised Superfluid nuclear model [10],

$$\rho(U) = \rho_{qp}(U') K_{vib}(U') K_{rot}(U') \tag{3}$$

here $\rho_{qp}(U')$ denotes density of quasi particle nuclear excitation. The terms $K_{rot}(U')$ and $K_{vib}(U')$ are the rotational and vibrational enhancement factors at effective energy of excitation U' , respectively [8].

Results and Discussion

The excitation functions of nucleon induced reactions of ^{55}Mn target nucleus as a function of projectile energy have been calculated using ALICE/ASH code [8] for the Hybrid

[14, 15], Geometry Dependent Hybrid [13] and Weisskopf Ewing models [12]. ALICE/ASH code provides the various alternative models for the determination of the level density. In calculations, the different nuclear level density models were used to obtain better fitting between measured data and theoretical results. In addition, “A/7” and “A/11” values for level density parameter in the FGM level density model by Geometry Dependent Hybrid model were selected. The level density parameter “ $a = A/11$ ” value at the other model calculations was used.

$^{55}\text{Mn}(n,4n)^{52}\text{Mn}$ Nuclear Reaction Cross Sections

Figure 1 shows the results of the model calculations, together with data measured by Uwamino et al. [17] for $^{55}\text{Mn}(n,4n)^{52}\text{Mn}$ reaction. In general, the experimental cross section values reported by Uwamino et al. [17] for the considered nuclear reaction are in good agreement with the obtained calculation results using FGM (Hybrid model) and FGM with $a = A/11$ (Geometry Dependent Hybrid model). The KRM level density model of Geometry Dependent Hybrid model predicts the nuclear cross sections lower than other models at investigated energy region. The excitation functions for this reaction increase rapidly with the increasing particle energy at considered energy range (Fig. 1).

$^{55}\text{Mn}(n,2p)^{54}\text{V}$ Nuclear Reaction Cross Sections

Figure 2 presents the ALICE/ASH calculations and TENDL-2014 data [18], together with data measured by

Lulic et al. [19] and Bramlitt and Fink [20] for $^{55}\text{Mn}(n,2p)^{54}\text{V}$ nuclear reaction. The cross section data reported by Lulic et al. [19] (0.11 mb at 14.6 MeV) and Bramlitt and Fink [20] (0.3 mb at 14.7 MeV) give different results to each other for this nuclear reaction. On the other hand, the model calculations by ALICE/ASH code give cross sections at incident energies above ~ 18 MeV. Generally, the Weisskopf Ewing model calculations and TENDL-2014 data are close to each other up to 40 MeV (Fig. 2). According to predictions based on ALICE code, the maximum cross section is 24.2 mb at incident energy 35 MeV by the KRM level density model of Geometry Dependent Hybrid model.

$^{55}\text{Mn}(n,^3\text{He})^{53}\text{V}$ Nuclear Reaction Cross Sections

The Hybrid, Geometry Dependent Hybrid and Weisskopf Ewing model cross section calculations, and TENDL-2014 (TALYS based) data, and the experimental data measured by Diksic et al. [21], Frevert [22] and Bramlitt et al. [23] are presented in Fig. 3. The experimental data measured by Frevert [22] have different values from cross section results of Diksic et al. [21] and Bramlitt et al. [23] for $^{55}\text{Mn}(n,^3\text{He})^{53}\text{V}$ reaction. The equilibrium and pre-equilibrium calculations via ALICE code give cross sections at energies above ~ 16 MeV. The obtained cross section data with different level density parameters in the FGM level density model by Geometry Dependent Hybrid model are in good agreement with each other. According to calculations based on ALICE code, the maximum cross section

Fig. 1 ALICE/ASH calculations (Hybrid, Geometry Dependent Hybrid and Weisskopf Ewing models) and experimental cross sections [17] for $^{55}\text{Mn}(n,4n)^{52}\text{Mn}$ nuclear reaction

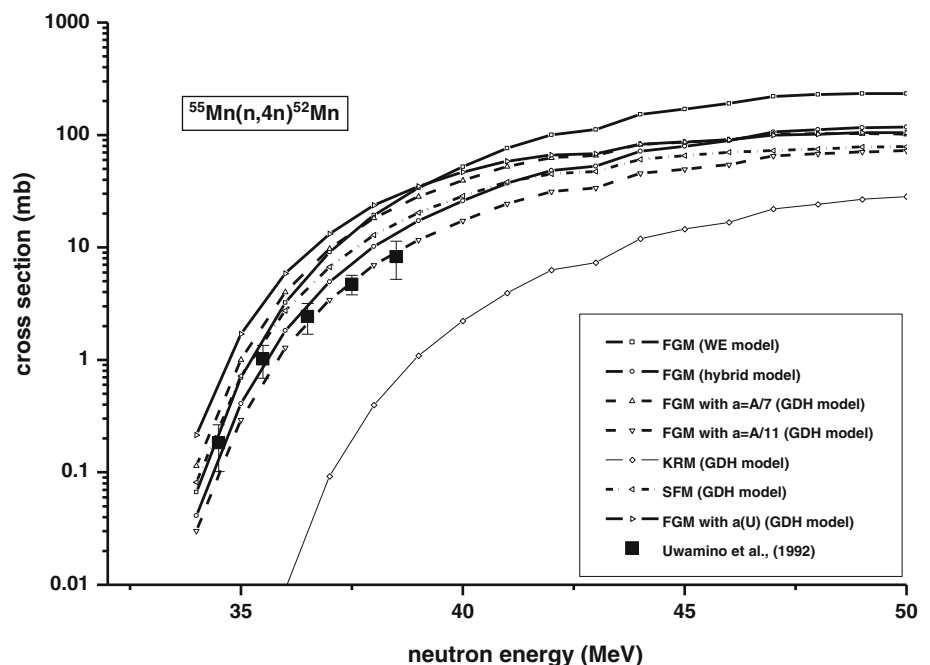


Fig. 2 TENDL-2014 data (TALYS-based), ALICE/ASH calculations (Hybrid, Geometry Dependent Hybrid and Weisskopf Ewing models) and experimental cross sections [19, 20] for $^{55}\text{Mn}(n,2p)^{54}\text{V}$ nuclear reaction

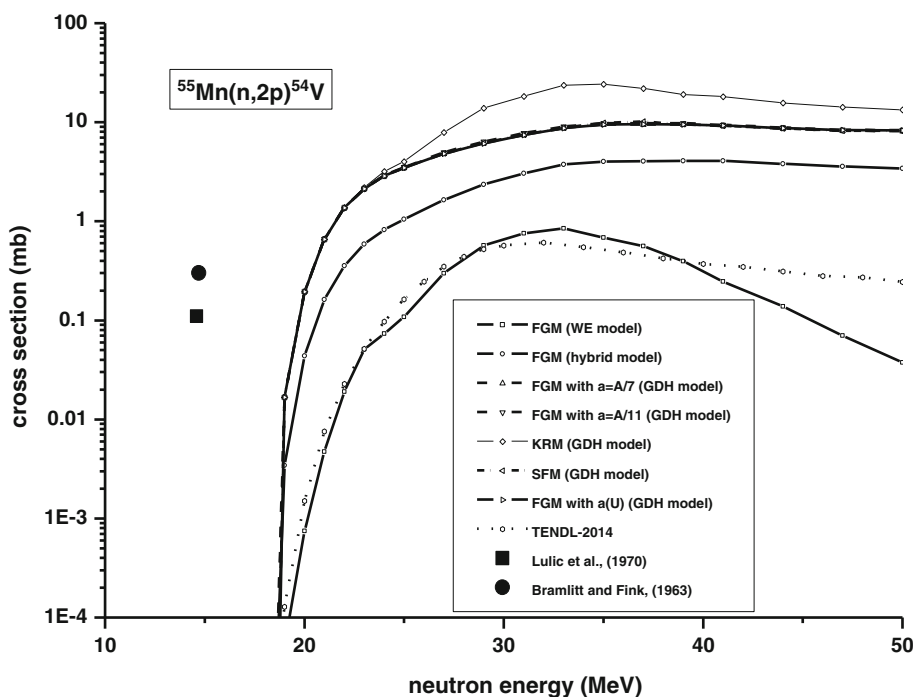
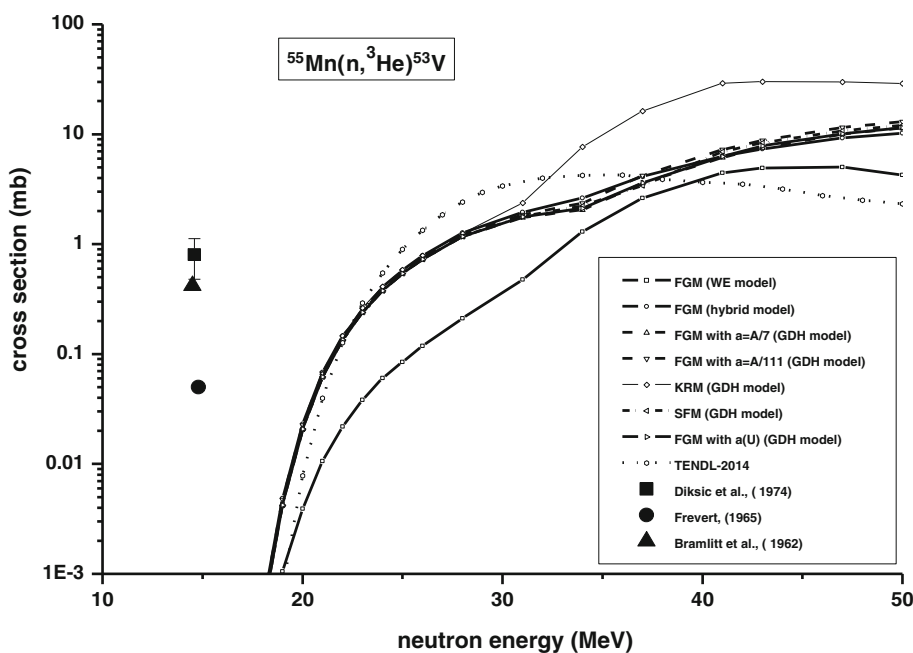


Fig. 3 TENDL-2014 data (TALYS-based), ALICE/ASH calculations (Hybrid, Geometry Dependent Hybrid and Weisskopf Ewing models) and experimental cross sections [21–23] for $^{55}\text{Mn}(n,^3\text{He})^{53}\text{V}$ nuclear reaction



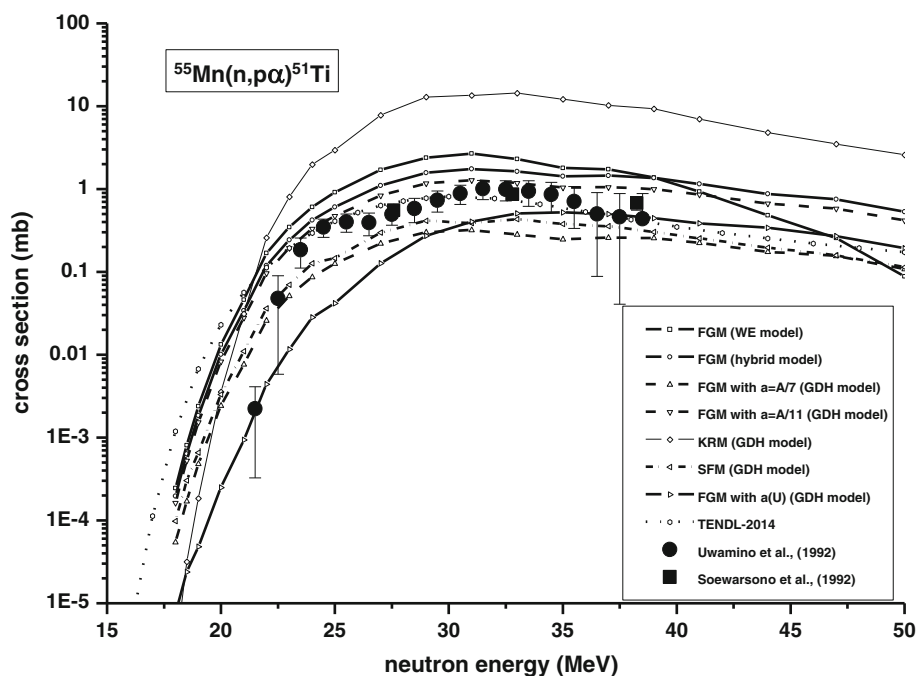
value is 30.07 mb at incident energy 43 MeV by the KRM level density model of Geometry Dependent Hybrid model.

$^{55}\text{Mn}(n, p\alpha)^{51}\text{Ti}$ Nuclear Reaction Cross Sections

TENDL-2014 data, the model calculations, and the experimental cross sections of Soewarsono et al. [24] and Uwamino et al. [17] for the nuclear reaction

$^{55}\text{Mn}(n,p\alpha)^{51}\text{Ti}$ are plotted in Fig. 4 as a function of projectile neutron energies. At maximum region of the excitation functions, the obtained cross section data with KRM level density model of Geometry Dependent Hybrid model are somewhat higher compared to the other data. TENDL-2014 data for this nuclear reaction agree with the the cross section data reported by Soewarsono et al. [24] and Uwamino et al. [17] within the error bars, except for the

Fig. 4 TENDL-2014 data (TALYS-based), ALICE/ASH calculations (Hybrid, Geometry Dependent Hybrid and Weisskopf Ewing models) and experimental cross sections [17, 24] for $^{55}\text{Mn}(n,p\alpha)^{51}\text{Ti}$ nuclear reaction



measured cross sections at the two incident energy of 21.5–22.5 MeV by Uwamino et al. [17].

$^{55}\text{Mn}(p,2n)^{54}\text{Fe}$ Nuclear Reaction Cross Sections

The calculated excitation curves for the investigated nuclear reaction are presented in Fig. 5. The obtained theoretical predictions using different level density models by ALICE/ASH code, and TENDL-2014 data for

considered nuclear reaction give maximum cross section values about projectile proton energy 15–25 MeV. Particularly, the cross section calculations with FGM (with $a(U)$) and KRM of Geometry Dependent Hybrid model by ALICE/ASH code give different results from other excitation functions at low energies. Weisskopf Ewing model-based calculations by ALICE/ASH code give the lowest cross sections for this nuclear reaction above 35 MeV (Fig. 5).

Fig. 5 TENDL-2014 data (TALYS-based) and ALICE/ASH calculations (Hybrid, Geometry Dependent Hybrid and Weisskopf Ewing models) for $^{55}\text{Mn}(p,2n)^{54}\text{Fe}$ nuclear reaction

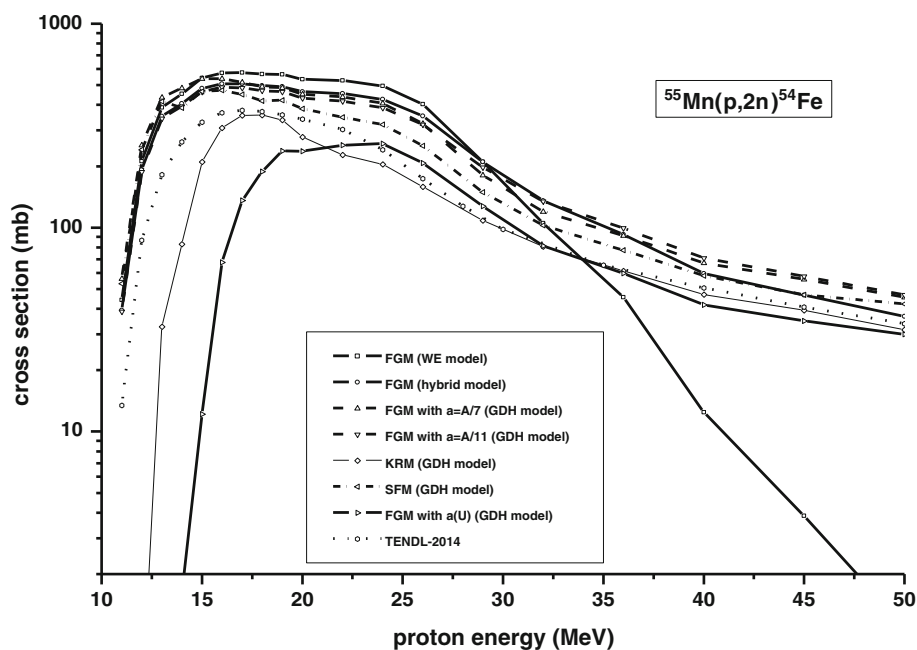
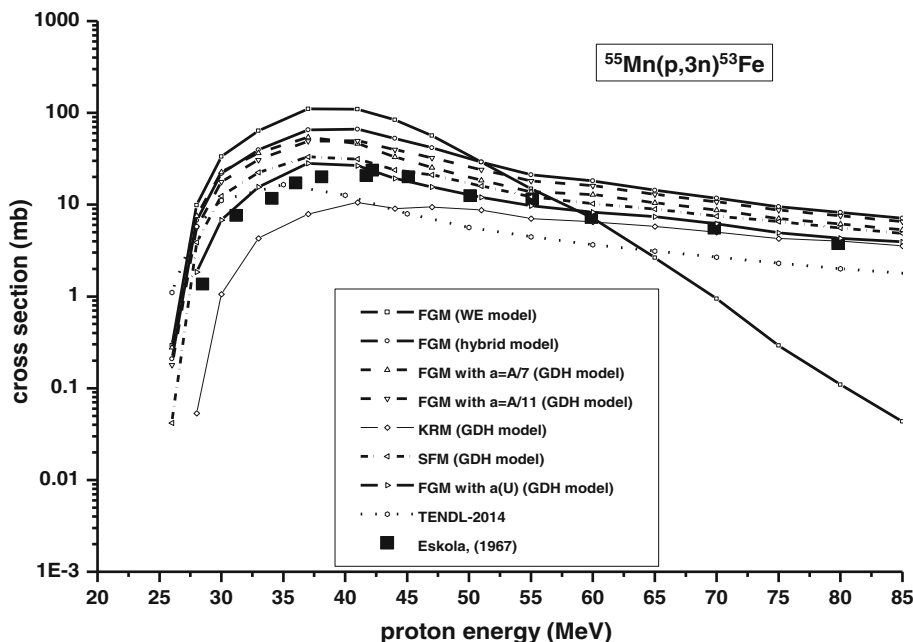


Fig. 6 TENDL-2014 data (TALYS-based), ALICE/ASH calculations (Hybrid, Geometry Dependent Hybrid and Weisskopf Ewing models) and experimental cross sections [25] for $^{55}\text{Mn}(p,3n)^{53}\text{Fe}$ nuclear reaction

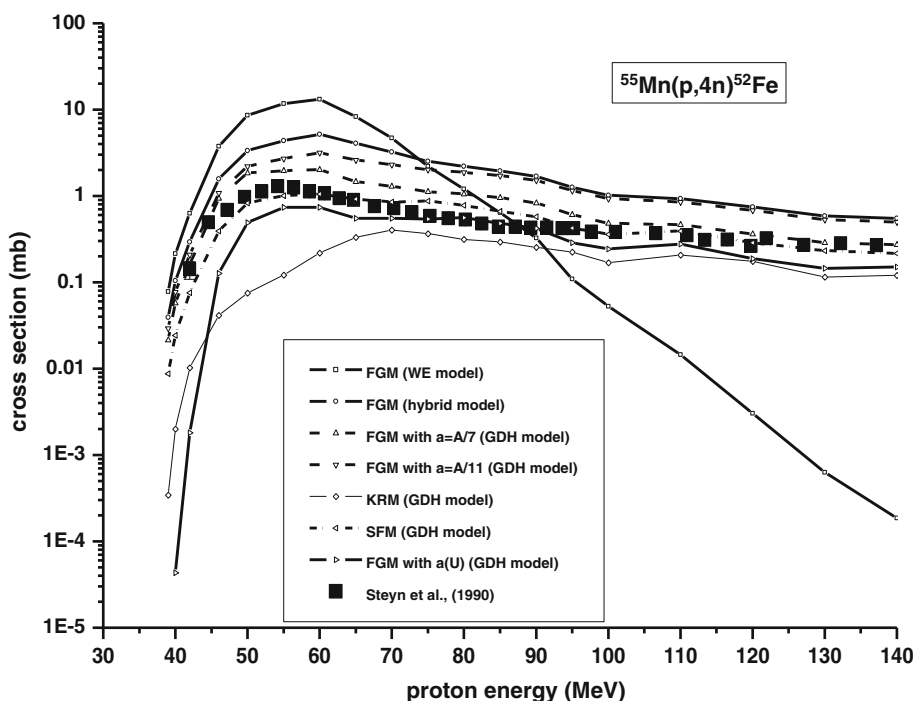


$^{55}\text{Mn}(p,3n)^{53}\text{Fe}$ Nuclear Reaction Cross Sections

The calculated excitation curves, and experimental data of Eskola [25] for the considered nuclear reaction are showed in Fig. 6 up to the incident proton energy of 85 MeV. It seemed that the measured experimental data by Eskola [25] are in good agreement with the FGM (with $a(U)$) of Geometry Dependent Hybrid model by

ALICE/ASH code. TENDL-2014 data, and the equilibrium and pre-equilibrium calculations by ALICE/ASH code, and the experimental data of Eskola [25] for considered nuclear reaction give maximum cross section values about projectile proton energy 35–55 MeV. The model-based calculations via Weisskopf Ewing model have the lowest cross sections for investigated nuclear reaction above 65 MeV energy.

Fig. 7 ALICE/ASH calculations (Hybrid, Geometry Dependent Hybrid and Weisskopf Ewing models) and experimental cross sections [26] for $^{55}\text{Mn}(p,4n)^{52}\text{Fe}$ nuclear reaction



$^{55}\text{Mn}(p,4n)^{52}\text{Fe}$ Nuclear Reaction Cross Sections

Figure 7 shows the equilibrium and pre-equilibrium calculations compared to the experimental cross sections of Steyn et al. [26] for $^{55}\text{Mn}(p,4n)^{52}\text{Fe}$ nuclear reaction. The experimental cross sections of Steyn et al. [26] are in good agreement with the SFM of Geometry Dependent Hybrid model by ALICE/ASH code. According to calculations based on ALICE code, the maximum cross section value for this reaction is 13.17 mb at incident energy of 60 MeV by the Weisskopf Ewing model. The obtained excitation function calculations using Weisskopf Ewing model have the lowest cross sections above energy of 95 MeV for this nuclear reaction.

Conclusions

In the present work, the nuclear cross sections of $^{55}\text{Mn}(n,4n)^{52}\text{Mn}$, $^{55}\text{Mn}(n,2p)^{54}\text{V}$, $^{55}\text{Mn}(n,^3\text{He})^{53}\text{V}$, $^{55}\text{Mn}(n,p\alpha)^{51}\text{Ti}$, $^{55}\text{Mn}(p,2n)^{54}\text{Fe}$, $^{55}\text{Mn}(p,3n)^{53}\text{Fe}$ and $^{55}\text{Mn}(p,4n)^{52}\text{Fe}$ reactions were calculated using the different nuclear models in the ALICE/ASH code. Finally, the results of calculations using the Geometry Dependent Hybrid model are in good agreement with experimental cross section data except for $^{55}\text{Mn}(n,2p)^{54}\text{V}$ and $^{55}\text{Mn}(n,^3\text{He})^{53}\text{V}$ nuclear reactions. However, the Weisskopf Ewing model cross section calculations including equilibrium process of nuclear reaction have the discrepancies with experimental data for the investigated energy region. It seemed that the nuclear cross section calculations are quite sensitive to level densities for nucleon induced reactions. Thereby, a fairly good prediction of the nuclear

cross sections can be obtained with selecting the suitable nuclear models and parameters in the reaction model code ALICE/ASH.

References

1. E.E. Bloom et al., J. Nucl. Mater. **329–333**, 12–19 (2004)
2. M. Yiğit et al., J. Fusion Energy. **32**, 317–321 (2013)
3. Y. Zhang et al., Rad. Phys. Chem. **81**, 1563–1567 (2012)
4. M. Yiğit et al., J. Fusion Energy. **32**(3), 362–370 (2013)
5. E. Tel et al., J. Fusion Energy. **32**(5), 531–535 (2013)
6. H. Özdoğan et al., J. Fusion Energy. **34**, 379–385 (2015)
7. A.J. Koning et al., Nucl. Phys. A **810**, 13–76 (2008)
8. C.H.M. Broeders et al., ALICE/ASH manual, FZK 7183, May 2006, <http://bibliothek.fzk.de/zb/berichte/FZKA7183.pdf>
9. A.V. Ignatyuk et al., Sov. J. Nucl. Phys. **21**, 255 (1975)
10. A.V. Ignatyuk et al., Yadernaja Fizika **29**, 875 (1979)
11. S.K. Kataria et al., Nucl. Instrum. Methods Phys. Res. Sect. A **288**, 585–588 (1990)
12. V.F. Weisskopf, D.H. Ewing, Phys. Rev. **57**, 472 (1940)
13. M. Blann, H.K. Vonach, Phys. Rev. C **28**, 1475–1492 (1983)
14. M. Blann, Phys. Rev. Lett. **28**, 757–759 (1972)
15. M. Blann, Phys. Rev. Lett. **27**, 337–340 (1971)
16. M. Blann, *ALICE-91; RSIC Code Package PSR-146* (Lawrence Livermore National Laboratory, California, 1991)
17. Y. Uwamino et al., Nucl. Sci. Eng. **111**, 391 (1992)
18. A. J. Koning et al., TALYS-based evaluated nuclear data library (2014) <ftp://ftp.nrg.eu/pub/www/talys/tendl2014/tendl2014.html>
19. S. Lulic et al., Nucl. Phys. A **154**(2), 273–282 (1970)
20. E.T. Bramlitt, R.W. Fink, Phys. Rev. **131**, 2649 (1963)
21. M. Diksic et al., J. Inorg. Nucl. Chem. **36**, 477 (1974)
22. E. Frevert, Acta Phys. Austriaca **20**, 304 (1965)
23. E.T. Bramlitt et al., Phys. Rev. **125**, 297 (1962)
24. T.S. Soewarsono et al., JAERI-M-92 Reports 027, 354 (1992)
25. K. Eskola, Ann. Acad. Sci. Fenn. Ser. A6. Physica **261**, 7 (1967)
26. G.F. Steyn et al., Appl. Radiat. Isot. **41**, 315–325 (1990)